

1995

*See 7/14*  
*11/1/95*

**NASA SUMMER FACULTY FELLOWSHIP PROGRAM**

**MARSHALL SPACE FLIGHT CENTER  
THE UNIVERSITY OF ALABAMA IN HUNTSVILLE**

**LINEARIZATION OF AN ANNULAR IMAGE BY USING A DIFFRACTIVE OPTIC**

Prepared By:	Donald R. Matthys, Ph. D.
Academic Rank:	Professor
Institution and Department:	Marquette University, Milwaukee, WI Department of Physics
NASA/MSFC:	
Office:	Astrionics
Division:	Optics and Radio Frequency
Branch:	Optical Design
MSFC Colleague	Helen J. Cole, Ph. D.



## Linearization of an Annular Image by Using a Diffractive Optic

In 1984, Dr. Pal Greguss of Hungary patented a side-viewing panoramic viewing system which consists of a single piece of glass with spherical surfaces which produces a 360 degree view of the region surrounding the lens which extends about 25 degrees in front of the lens and 20 degrees behind it. This belt-shaped region is imaged into an annular shaped virtual image within the lens; by using a standard lens as a transfer lens, this virtual image can be placed onto an optical sensor (film, camera, detector, eye) as a real image. Earlier efforts to obtain panoramic viewing go back at least to 1878 when Mangin obtained a patent for such a system. However, all of the earlier systems were either complex designs with many lenses, or blocks with non-spherical surfaces, or produced images of very poor quality. Thus almost all imaging of interior walls of cavities or panoramic views were obtained by using traditional lenses and simply rotating the system about an axis. Greguss' system is simple, easy to fabricate, and produces images of good quality. Another useful property of the lens is that it is essentially afocal, *i.e.*, images stay in focus for objects located right next to the lens as well as for objects located far away from the lens.

The lens designed by Greguss produced a panoramic view in an annular shaped image, and so the lens was called a PAL (panoramic annular lens). The physical shape of the PAL is shown in Figure 1, which also shows a few rays from a cylindrical wall surrounding the PAL and coaxial with it. Note that the central region of the PAL is not used and that sections of the front and back sides of the lens are coated and used as mirrors. These mirrored surfaces are shown in Figure 1 as thick heavy lines. Note also the location of the virtual image within the lens and the use of a transfer lens to produce a real image.

Figure 2 shows a different view of the PAL inside a cylindrical cavity and indicates how the final image is shaped like an annulus. The images produced by this system are of necessity distorted, since a curved surface (cavity wall) cannot be represented on a flat surface (real image) without introducing some distortion. However, the distortion is relatively minor, and viewers of the image have no difficulty interpreting it. Indeed, the image is of sufficient quality to allow standard holographic interferometric and electronic speckle pattern interferometric measurements of minute displacements of the cavity surface.

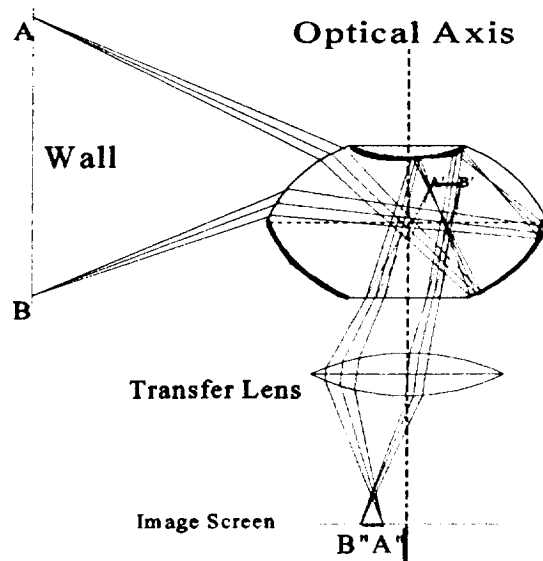


**Figure 1.** Ray diagram for a PAL located within a cylinder, showing the virtual image transferred to a screen by a lens.

When applying these traditional measurements to PAL images, it is found advantageous to linearize the annular image, *i.e.*, to transform the annulus into a rectangle which looks like the belt shaped region of the imaged cavity wall as if it were opened flat. This can easily be done with a computer and such a linearized image can be produced within about 40 seconds on current microcomputers. However, this process requires a frame-grabber and a computer, and is not real-time.

Therefore, it was decided to try to perform this linearization optically by using a diffractive optic. The final

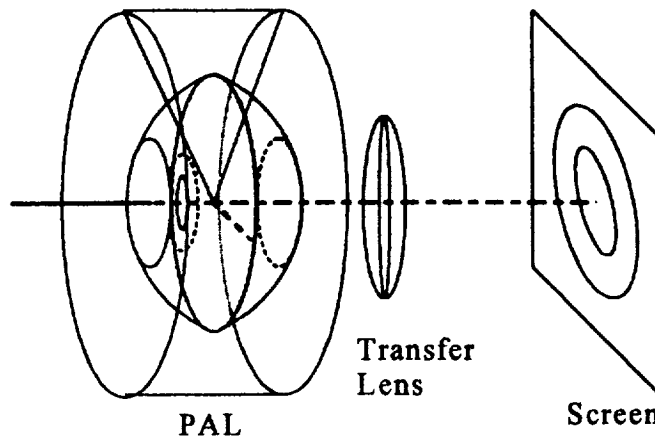


Figure 2. Another view of a PAL showing how the annular image is produced.

image would then be obtained in real-time and requires no additional equipment

mask, the continuous phase could be approximated modulo  $2\pi$  with stepwise changes. A single mask allowed 2 levels in the approximation, two masks allowed 4 levels, three masks 8 levels, and four masks 16 levels. With the higher number of masks came much higher efficiency: a two level approximation gave only about 30 per cent efficiency, while 16 levels could give over 95 per cent efficiency.

Thus diffractive lenses of high efficiency could be used for transforming images if methods for introducing a variable grating spacing to match the varying phase shifts needed could be devised.

Designs were quickly found for the production of simple diffractive lenses that could compensate for some of the aberrations of traditional lenses, and the new diffractive elements offered additional advantages in weight and use of material; indeed, in some cases the desired gratings could be cut right into the surface of the refractive lens the new lens was to complement.

However, the design of complex systems for producing diffractive elements that might perform unique functions unobtainable from traditional lenses is more challenging. In the project described in this report, an annular image was to be modified into a rectangular image, and the distortions in the annular image compensated. A formalism to determine the phase map required to change the geometric characteristics of the original image had to be developed. Assuming the original image in the x-y plane was covered with a variable grating, the location of each point in the image was to be mapped to some point in the u-v plane. Limiting the discussion to one dimension, assuming the small angle approximation  $\theta = \sin \theta = \tan \theta$ , applying the grating equation  $a \sin \theta = \lambda$  where  $a$  is the grating spacing, and expressing quantities in terms of spatial frequencies, gives  $\theta = \lambda/a = (2\pi/k)/(2\pi/q)$  where  $q$  is the angular spatial frequency of the grating in radians/distance. Since the link between phase and spatial frequency is given by  $q = d\phi/dx$ , examination of Figure 3 shows that the phase map  $\phi(x) = (k/d)[\int u(x) dx - x^2/2]$ . The last term in this equation describes the phase shift introduced by a simple refractive lens and so will be dropped and replaced physically by a lens of focal length  $f = d$ .

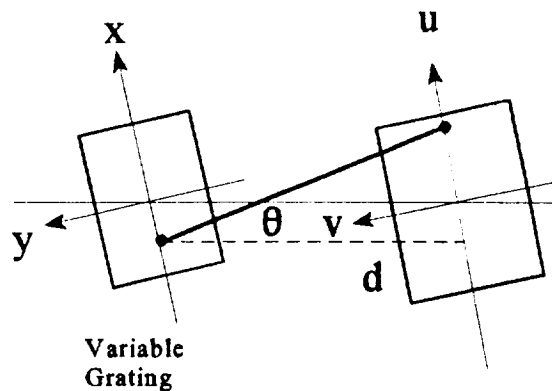


**Figure 3.** Transformation of a point in the x-y plane to a point in the u-v plane;  $u = f(x)$ , the two planes are separated by  $d$ , and it is desired to determine the grating frequency  $q$  which will produce the necessary angle  $\theta$ .

Going to two dimensions is straightforward, and for the case under study the transformations are  $u(x,y) = x_0 \ln ([x^2 + y^2]^{1/2})$  and  $v(x,y) = x_0 \operatorname{atan}(y/x)$ , where  $x_0$  is an arbitrary scale factor having the dimension of length. The application of these transforms is shown in Figure 4 and the desired phase function is  $\phi(x,y) = (kx_0/d) \{ \ln ([x^2 + y^2]^{1/2}) - y \operatorname{atan}(y/x) - x \}$ . Once the requisite mathematical formalism has been found, it is put into a

computer, the phase map is generated, the desired contours of fixed phase are determined, and a fracturing algorithm is applied to produce the desired phase mask for the transformation. The procedure used to fracture the data is shown in Figure 5. In Figure 5 an arbitrary point P1 is chosen on the contour curve and its gradient is found, which then gives the normal and the tangent lines to the contour curve.

Another arbitrary point P2 is then chosen and its gradient found. When the intersection P3 is found for the two tangent lines through P1 and P3, the error between P3 and the contour value is measured. If this is smaller than the allowed maximum error, point P2 is moved further away and the process is repeated. If the error is too large, P2 is moved closer. The width of the rectangles is determined by moving down the perpendicular to the contour line until the phase change desired is attained. This process is repeated for each pair of contour lines specifying a zone. When the appropriate zones over the phase map have all been fractured and filled by the rectangles, the resulting list of rectangles is fed to a photolithographic machine which actually produces the desired phase mask

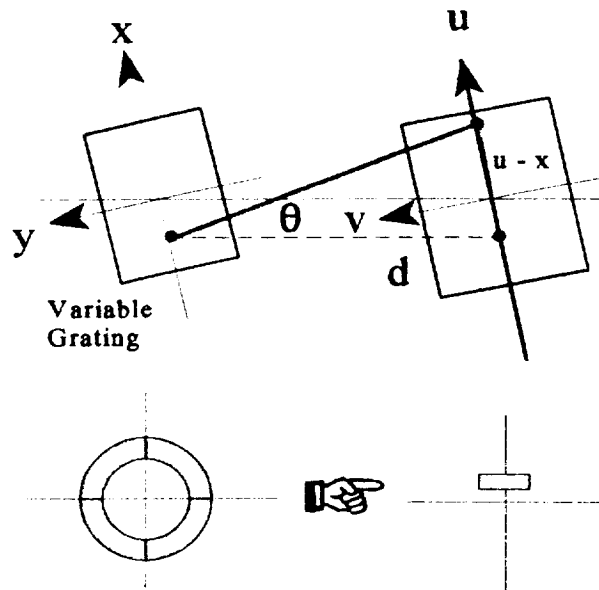


**Figure 4.** Diagram showing a log-polar transformation, where the coordinate transforms are  $u(x,y) = x_0 \ln ([x^2 + y^2]^{1/2})$  and  $v(x,y) = x_0 \operatorname{atan}(y/x)$ . The upper figure shows the geometric relationships and the lower figure shows the effect of the transform on the annular image.

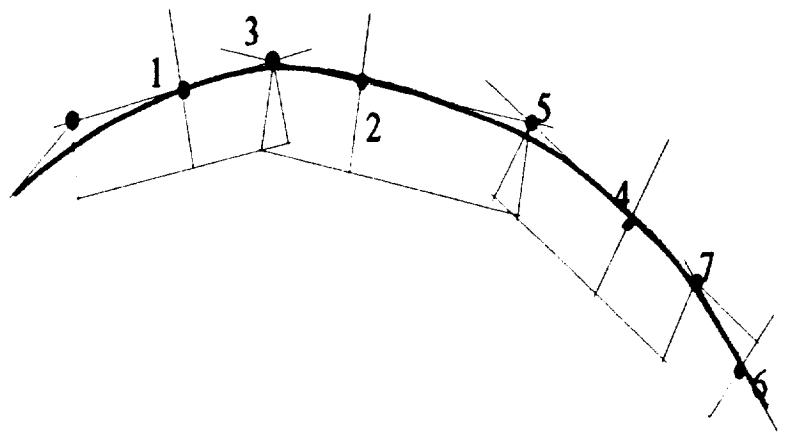


**Figure 5.** Diagram showing how the region defined by specified curved contour lines is approximated by rectangles.

for the diffractive optic. This mask is used to expose a properly prepared substrate and the mask pattern is etched into the substrate to actually produce the desired diffractive optic.

Once the diffractive optic has been produced, the setup shown in Figure 6 is used to produce the modified image. Since the diffractive element has no imaging power and the light into it must be collimated, the image to be transformed is placed on an LCD display which essentially presents it as a transparency to the incoming light. After going through the image, the light passes through the diffractive optic and a focussing lens which produce an image at  $f = d$  from the lens. This image is very small since the LCD screen is less than two inches high and the scaling factor is between 0.2 and 0.4. Also, since there is only a single two level diffractive element, the efficiency is very low (about 30 per cent). Finally, the low resolution of the TV display blurs the image. In sum, the final transformed image is of very poor quality. If it is really desired to produce a sharp image, then an element of at least eight levels should be made, and an LCD display of at least 300 by 300 pixels should be used. Recall that for this project the real goal was to develop the algorithms for fracturing the zones defined by the mapping transformation, and to actually produce the binary optic in an appropriate setup. These goals were both obtained.

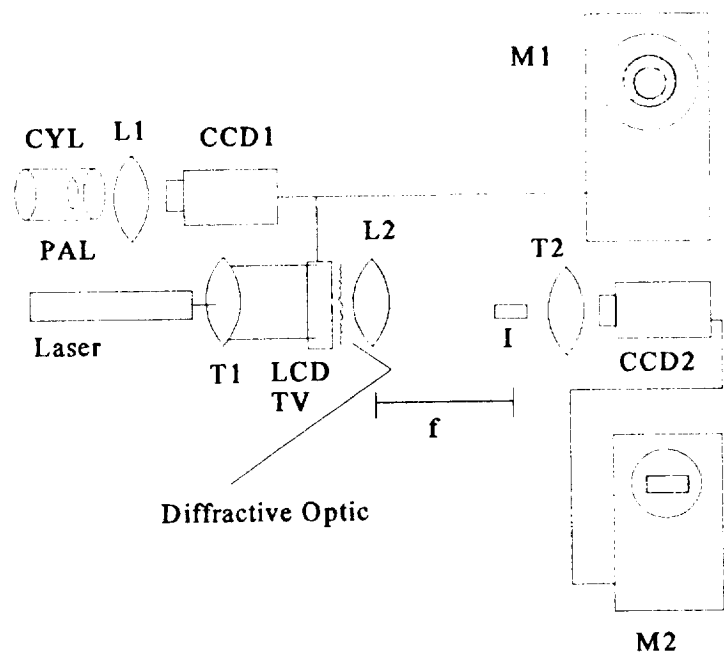


**Figure 6.** Layout for viewing the log-polar transformation. CYL cylindrical pipe; PAL panoramic lens; L1, L2 lenses; T1, T2 telescope expanders; M1, M2 monitors; I real image; CCD1, CCD2 cameras;  $f$  design focal length of diffractive optic. Monitor 1 shows annular image from PAL, monitor 2 shows image after transformation.

### Bibliography

1. Matthys, Gilbert, Greguss, "Endoscopic Measurement using Radial Metrology with Digital Correlation", *Optical Engineering* **30** (10), 1455-1460, 1991.
2. Swanson, G.J., "Binary Optics Technology: Theory and Design of Multi-Level Diffractive Optical Elements", Lincoln Laboratory, Massachusetts Institute of Technology, Technical Report 854, August 14, 1989.
3. Saleh, Freeman, "Optical Transformations", in *Optical Signal Processing*, ed. by J. Horner. Academic Press 1987.

